

Anomalous force-velocity relation of driven inertial tracers in steady laminar flows

F. Cecconi¹, A. Puglisi¹, A. Sarracino¹, and A. Vulpiani^{2,3}

¹ CNR-ISC and Dipartimento di Fisica, Sapienza Università di Roma, p.le A. Moro 2, 00185 Roma, Italy

² Dipartimento di Fisica, Sapienza Università di Roma, and CNR-ISC, p.le A. Moro 2, 00185 Roma, Italy

³ Centro Interdisciplinare B. Segre, Accademia dei Lincei

Received: date / Revised version: date

Abstract. We study the nonlinear response to an external force of an inertial tracer advected by a two-dimensional incompressible laminar flow and subject to thermal noise. In addition to the driving external field F , the main parameters in the system are the noise amplitude D_0 and the characteristic Stokes time τ of the tracer. The relation velocity vs force shows interesting effects, such as negative differential mobility (NDM), namely a non-monotonic behavior of the tracer velocity as a function of the applied force, and absolute negative mobility (ANM), i.e. a net motion against the bias. By extensive numerical simulations, we investigate the phase chart in the parameter space of the model, (τ, D_0) , identifying the regions where NDM, ANM and more common monotonic behaviors of the force-velocity curve are observed.

PACS. 05.40.-a Fluctuation phenomena, random processes, noise, and Brownian motion – 05.45.-a Non-linear dynamics and chaos

1 Introduction

The study of the transport properties of inertial particles in fluids takes on a great importance in several fields, in engineering as well as in natural occurring settings: typical examples are pollutants and aerosols dispersion in the atmosphere and oceans [1], optimization of mixing efficiency in different contexts, or the study of chemical [2], biological [3] or physical interaction [4], with applications to the time scales of rain [5], in the sedimentation speed under gravity [6], or to the planetesimal formation in the early Solar System [7].

Under external perturbations, the dynamics of tracer particles can be significantly modified, resulting in different behaviors which are not easily predicted from the properties of the unperturbed dynamics. In order to relate response functions and fluctuations in non-equilibrium conditions, relevant in the aforementioned cases, generalizations of the standard fluctuation-dissipation theorem have been derived in recent years [8,9,10,11,12,13]. These approaches are generally valid in the small forcing limit, and a central problem remains the study of the motion in the presence of an external driving field F , in the nonlinear regime. In this case, the particles reach a stationary state characterized by a finite average velocity v which non-trivially depends on the system parameters. The main point is then to understand the force-velocity relation $v(F)$, which contains relevant information on the system. These curves are strongly affected by the nature of the tracer/fluid interaction, and can show surprising nonlinear behaviors.

An example of such effects is provided by the so-called negative differential mobility (NDM), which means that $v(F)$, after a linear increase with the applied force, can show a non-monotonic behavior, attaining a (local) maximum for a given value of the force [14,15,16,17,18,19]. For larger intensity of the bias the velocity can show different behaviors, such as saturation or asymptotic linear growth, depending on the considered model. In other situations, one can also observe a more surprising feature: an *absolute* negative mobility (ANM), where the particle travels on average against the external field [20,21,22,24]. In general, these non-linear behaviors are due to trapping mechanisms in the system, which lead to dynamical conditions such that an increase of the applied force can result in an increase of the trapping time, and, consequently, to a slowing down of the average tracer dynamics. Depending on the specific model, trapping can be due to the interaction of the tracer with the surrounding particles, to frustration in the system, to geometric constraints or to the coupling with underlying velocity fields.

Here we study the response to an external bias of inertial particles advected by steady (incompressible) cellular flows, in the nonlinear regime. In these systems, the presence of inertia induces a non-trivial deviation of the particle motion from the flow of the underlying fluid: the particles can remain trapped in regions close to upstream lines, yielding a slowing down of the dynamics, as observed in the context of gravitational settling [25,26,27,28], and typically leading to the phenomenon of preferential con-

centration [29,30]. In a recent work [31], we have considered a model where, in addition to the cellular flow and the external force, the inertial tracer is subject to the action of a microscopic (thermal) noise. We have shown that a rich nonlinear behavior for the average particle velocity can be observed, as a function of the applied force, featuring both NDM and ANM. The latter was never observed in the standard systems studied in the literature. Here we present an extensive numerical investigation of the system studied in [31], exploring a wide range of the model parameters and reconstructing the phase chart, where regions of NDM and ANM are identified.

2 The model

The dynamics of the inertial tracer in two dimensions, with spatial coordinates (x, y) and velocities (v_x, v_y) , is described by the following equations

$$\dot{x} = v_x, \quad \dot{y} = v_y \quad (1)$$

$$\dot{v}_x = -\frac{1}{\tau}(v_x - U_x) + F + \sqrt{2D_0}\xi_x, \quad (2)$$

$$\dot{v}_y = -\frac{1}{\tau}(v_y - U_y) + \sqrt{2D_0}\xi_y, \quad (3)$$

where $\mathbf{U} = (U_x, U_y)$ is a divergenceless cellular flow defined by a stream-function ψ as:

$$U_x = \frac{\partial\psi(x, y)}{\partial y}, \quad U_y = -\frac{\partial\psi(x, y)}{\partial x}. \quad (4)$$

Here τ is the Stokes time, F the external force, and

$$\psi(x, y) = LU_0/2\pi \sin(2\pi x/L) \sin(2\pi y/L). \quad (5)$$

ξ_x and ξ_y are uncorrelated white noises with zero mean and unitary variance. A pictorial representation of the field (red arrows) and of a tracer's trajectory (black arrows) is reported in Fig.1. Measuring length and time in units of L and L/U_0 respectively, and setting therefore $U_0 = 1$ and $L = 1$, the typical time scale of the flow becomes $\tau^* = L/U_0 = 1$. Let us anticipate that the time scales ratio τ/τ^* will play a central role in the behavior of the system. Another important parameter of our model is the microscopic thermal noise with diffusivity D_0 , which guarantees ergodicity and can be expressed in terms of the temperature T of the environment by the relation $D_0 = T/\tau$.

In the following we will focus on the force-velocity relation, namely on the behavior of the stationary velocity $\langle v_x \rangle = \tau F + \langle U_x[x(t), y(t)] \rangle$, where $\langle \dots \rangle$ denotes averages over initial conditions and noise realizations. The numerical integration of the dynamical equations of the model is performed with a second-order Runge-Kutta algorithm [32], with a time step $\Delta t = 10^{-2}$. Numerical results shown in the figures are averaged over about 10^4 realizations. In our study, we will consider different regimes of the time scale ratio τ/τ^* , exploring the behavior of the force-velocity relation $\langle v_x \rangle(F)$ by varying the microscopic diffusivity D_0 .

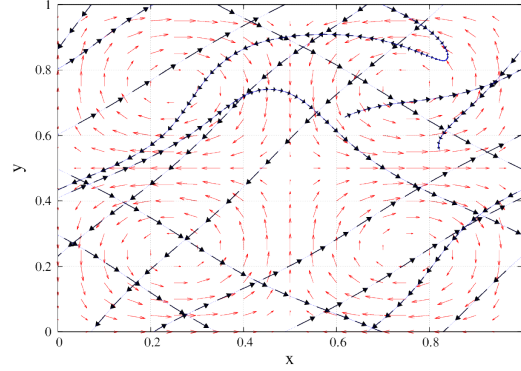


Fig. 1. Sample trajectory of an inertial particle (black arrows) advected by the underlying velocity field (red arrows), in the presence of external force and thermal noise, for parameters $\tau = 10$, $F = 10^{-2}$, $D_0 = 10^{-5}$.

3 Force-velocity relation

3.1 Small Stokes time

First, we consider the case $\tau \ll \tau^*$. Fig.2 shows $\langle v_x \rangle(F)$ for $\tau = 10^{-2}, 10^{-1}$ and different values of D_0 . Two linear regimes at small and large forces are well apparent. In the latter case, the simple behavior $\langle v_x \rangle(F) = \tau F$ is recovered. This is expected because at large forces the underlying velocity field is irrelevant. More surprisingly, in the range of intermediate forces a non-trivial nonlinear behavior takes place. In particular, a non-monotonic behavior, corresponding to NDM, can be observed for small values of D_0 . Note that the critical force value F^* where the abrupt drop of velocity occurs is independent of the noise amplitude and scales with τ as $F^* = \tau^{-1}$. As D_0 is increased, the effect of the velocity field is averaged out and the force-velocity curve displays a simple monotonic behavior.

This scenario is illustrated by Fig.3, showing trajectories of the tracer in the case $\tau = 0.01$ and $D_0 = 10^{-5}$, for some values of the force $F \in [1, 100]$ along with the streamlines of the effective flow obtained implementing a geometric singular perturbation approach in the Stokes time τ from the system with $\tau = 0$. According to Fenichel [33], for small τ , particle trajectories of the system are attracted by a two-dimensional slow manifold and the equations of motion along the manifold can be formally written as a perturbation series

$$\dot{x} = U_x(x, y) + F\tau + \sum_n \tau^n h_n(x, y) \quad (6)$$

$$\dot{y} = U_y(x, y) + \sum_n \tau^n k_n(x, y) \quad (7)$$

where the terms $\{h_n, k_n\}$ are explicitly derived in Refs. [26, 34]. Eqs. (6,7), also referred to as *inertial equations*, have the advantage of reducing the dimensionality of the system from four to two, yet catching the correct asymptotic behavior of full-system trajectories. The drawback lies in the obvious technical difficulties to control the convergence and in dealing with truncation errors. Let us

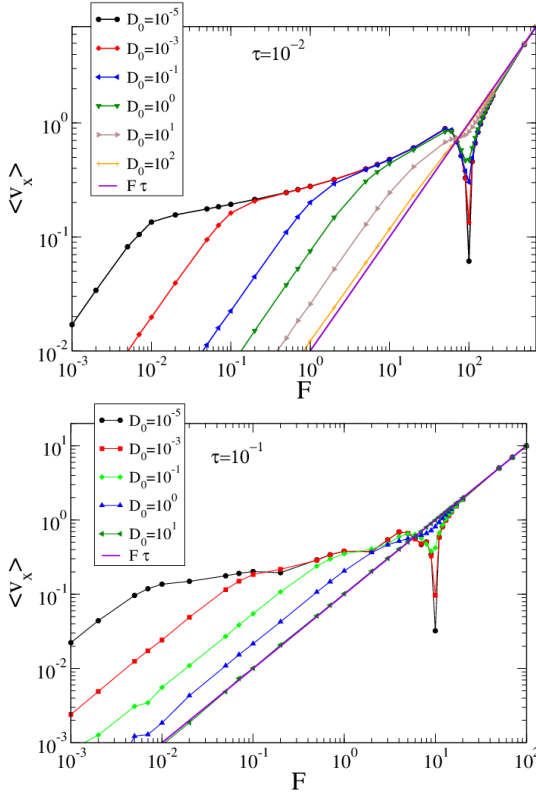


Fig. 2. Plot of $\langle v_x \rangle$ versus F several values of D_0 . Top panel refers to $\tau = 10^{-2}$, while bottom panel refers to $\tau = 10^{-1}$. Note the abrupt drops of the curves at the value $F = F^* = 1/\tau$.

note that such a limit is singular and, since now we are in two dimensions, chaos cannot exist. In our case, retaining only the 4-th order terms in τ in Eqs. (6,7) is sufficient to discuss the qualitative features of the trajectories on the slow manifold, see Fig.3. At small forces ($F = 1, 10, 50$), the asymptotic trajectories (black dots) accumulate along the main streamlines of the effective velocity field, following the external force. For larger values ($F = 70, 90, 100$), one observes an interesting phenomenon: the trajectories move towards upstream regions with respect to the external force, so that the inertial tracers slow their motion, decreasing the stationary average velocity.

3.2 Large Stokes time

In the opposite regime, $\tau \gg \tau^*$, we find a behavior similar to that discussed above, with NDM at small D_0 and monotonic behavior for $D_0 \geq 10^{-3}$, see Fig. 4. However, the drop in the velocity is much milder in this case, and the minimum is reached for $F \approx 7 \cdot 10^{-3}$. This behavior can be explained by the fact that, since inertia is larger in this case, the action of the velocity field is weaker and the effect of slowing down on the tracer is reduced.

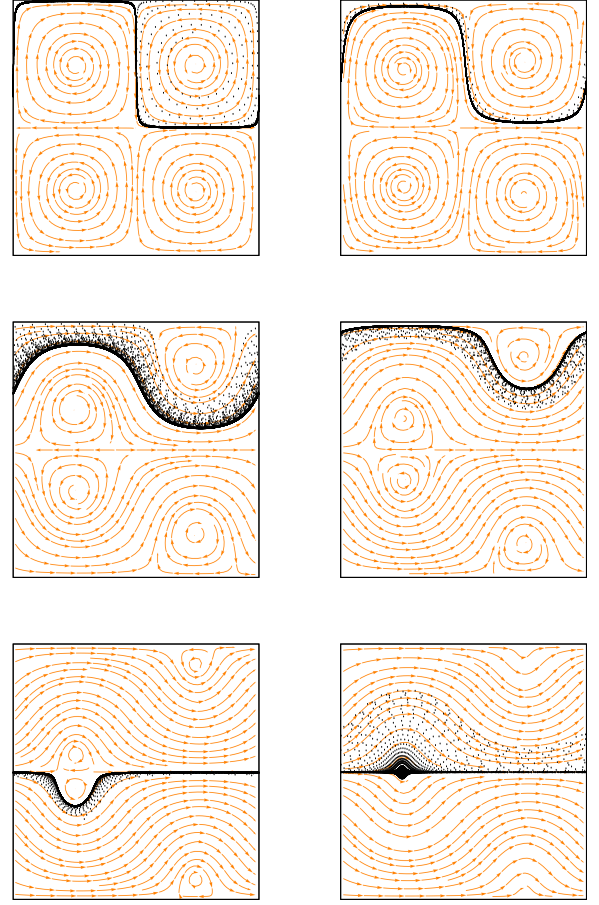


Fig. 3. Black dots represent trajectories of the full equations of motions (Eqs. (1)-(3)) for driven inertial tracer in the case $\tau = 0.01$ and $D_0 = 10^{-5}$, for some values of the force $F = 1, 10, 50, 70, 90, 100$ from left to right and from top to bottom. Orange arrows represent the streamlines of the effective flow in Eqs. (6)-(7), obtained implementing a geometric singular perturbation approach in the Stokes time τ from the system with $\tau = 0$.

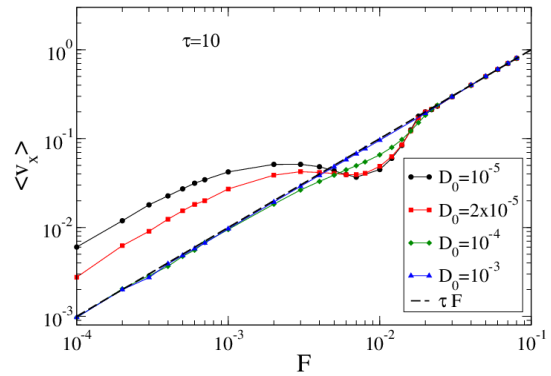


Fig. 4. Force-velocity relation for $\tau = 10$ and several values of D_0 .

3.3 Absolute negative mobility

If the relevant time scales of the tracer and of the underlying velocity field are comparable, $\tau \sim \tau^*$, a new surprising effect can be observed. In Fig. 5 we show $\langle v_x \rangle(F)$ for $\tau = 0.65$ (top panel) and $\tau = 0.8$ (bottom panel), and different values of D_0 . We observe a nonlinear complex behavior of the force-velocity relation and, in particular, we note that the average velocity can take on negative values, $\langle v_x \rangle < 0$ within the error bars, implying an absolute negative mobility of the tracer. This phenomenon occurs in a very narrow range of forces for small values of D_0 (see black dots in Fig. 5), while for values of $D_0 = 10^{-3}$ negative mobility extends at small forces, even in the linear regime (see green diamonds). This effect is made possible by the non-equilibrium nature of our model due to the non-gradient form of the velocity field (see Eq. (4)), which induces currents even in the absence of the external force.

In particular, our results seem to be consistent with the theoretical analysis presented in [35], for an underdamped Brownian particle model in a one-dimensional periodic potential. Indeed, it is expected that in some regions of the parameter space, at fixed force, the tracer velocity follows the external force for low noise, but changes sign upon increasing the temperature. A physical mechanism responsible for such a surprising effect has been proposed in [31], based on a careful study of the tracer trajectories. This analysis showed that the motion of the tracer is realized along preferential “channels”, aligned downstream or upstream with respect to the force. Transitions between channels are induced by the subtle interplay between inertia and thermal noise, analogously to the mechanism described in [22] for a model of a driven inertial Brownian particle moving in a periodic potential and subject to a periodic forcing in one dimension. In our case, the external force can induce a bias in such transitions, yielding an average $\langle v_x \rangle \neq 0$. In particular, we observed [31] that in a specific range of forces the tracer can be biased to visit more frequently upstream channels, slowing its motion, and leading to NDM or even to ANM. An analogous mechanism has been described in [23].

3.4 Phase chart

Our extensive numerical study of the model is summarized in the phase chart reported in Fig. 6. We identified three “phases”, corresponding to simple monotonic behavior (black dots), NDM (red squares) and ANM (blue triangles), for the velocity-force relation, in the parameter space (τ, D_0) . For each couple of parameters, we performed numerical simulations studying the curve $\langle v_x \rangle(F)$ and focusing on the regions where non-linear behaviors occur. As expected, for large values of the microscopic diffusivity D_0 , the system exhibits a simple behavior, because noise dominates over the effect of the underlying velocity field, and a monotonic behavior is observed. The same happens for large values of τ , when again the underlying field can be neglected. NDM seems a typical phenomenon

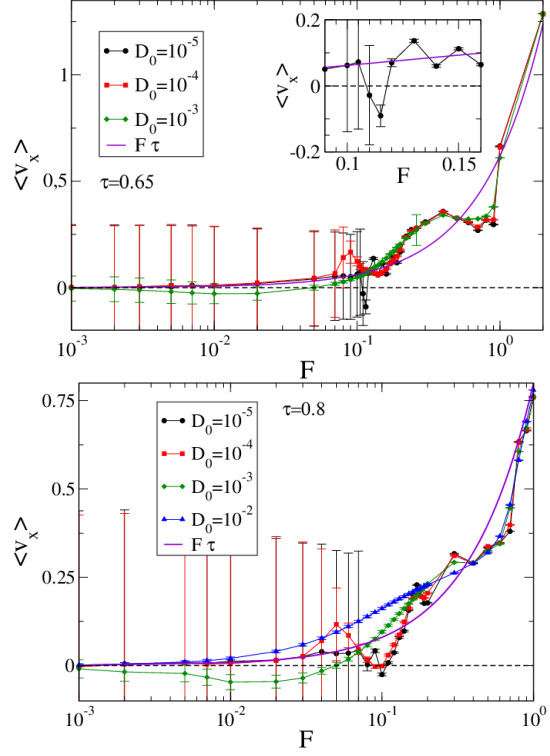


Fig. 5. Top panel: force-velocity relation for $\tau = 0.65$ and several values of D_0 . The inset shows a zoom of the ANM region. Bottom panel: force-velocity curve for $\tau = 0.8$ and several values of D_0 . The large error bars at small forces are due to the fact that, in those cases, the inertial particles are constrained along few straight trajectories, with opposite mean velocity, strongly dependent on the initial conditions. This effect produces a large variance.

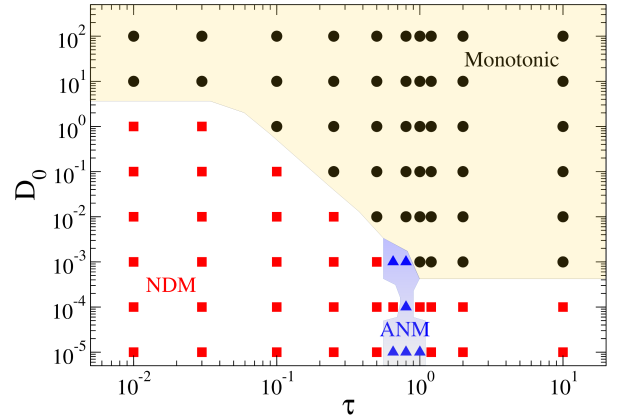


Fig. 6. Phase chart in the parameter space of the model. Black dots identify the region where monotonic behavior of the force-velocity relation is observed, red squares regions where NDM takes place, and blue triangles regions where ANM occurs.

for small values of τ and D_0 , where the different driving mechanisms acting on the tracer are comparable and

coupled, leading to non-monotonic behaviors. Our study also unveils a narrow region where ANM can be observed, which occurs for values of $\tau \sim \tau^*$, where τ^* is the typical time scale of the underlying velocity field. For $\tau \rightarrow 0$, the occurrence of ANM can be excluded due to the no-go theorem discussed in [35].

4 Conclusions

We have investigated a model for the dynamics of an inertial tracer advected by a laminar velocity field, under the action of an external force and subject to thermal noise. This model can be useful to describe the transport properties of small particles (e.g. soil dust, man-made pollutants or swimming microorganisms [36]) dispersed in fluids in different contexts, such as aerosol sedimentation, plankton concentration, or gravitational settling, with application in several areas of engineering, oceanography or meteorology.

We focused on the force-velocity relation of the tracer in the nonlinear forcing regime. The system shows a very rich phenomenology, featuring negative differential and absolute mobility, as summarized by the phase chart in the model parameter space. The emergence of these effects is due to the subtle coupling between the velocity field dynamics and the inertia of the tracer, and crucially depends on the amplitude of the microscopic thermal noise and on the time scale ratio between the tracer Stokes time and the characteristic time of the fluid. The presence of two non-equilibrium sources in the system, namely the non-gradient force and the external bias, and its combined action, make the model very rich: beyond the known trapping effects which result in a reduction of the tracer velocity upon increasing the applied force, in our model we also observe regions of negative mobility, where the particle travels against the external force. This phenomenon demands for experimental investigation in real systems.

Author contribution statement

All authors contributed equally to the paper.

References

1. J. H. Seinfeld, and N. S. Pandis. *Atmospheric chemistry and physics: from air pollution to climate change*. John Wiley & Sons, 2016.
2. V. Hessel, H. Löwe and F. Schönfeld, *Chem. Eng. Sci.* **60**, (2004) 2479.
3. W. M. Durham, E. Climent, M. Barry, F. De Lillo, G. Boffetta, M. Cencini, and R. Stocker, *Nature Commun.* **4**, (2013) 2148.
4. K. Gustavsson and B. Mehlig, *Adv. Physics*, **65**, (2016) 1.
5. G. Falkovich, A. Fouxon, and M.G. Stepanov, *Nature* **419**, (2002) 151.
6. F. De Lillo, F. Cecconi, G. Lacorata, and A. Vulpiani, *EPL* **84**, (2008) 40005.
7. A. Bracco, P. H. Chavanis, A. Provenzale, and E. A. Spiegel, *Phys. Fluids* **11**, (1999) 2280.
8. F. Corberi, E. Lippiello and M. Zannetti, *J. Stat. Mech.* (2007) P07002.
9. U. Marini Bettolo Marconi, A. Puglisi, L. Rondoni, and A. Vulpiani, *Phys. Rep.* **461**, (2008) 111.
10. E. Lippiello, F. Corberi, A. Sarracino, and M. Zannetti, *Phys. Rev. B* **77**, (2008) 212201.
11. E. Lippiello, F. Corberi, A. Sarracino, and M. Zannetti, *Phys. Rev. E* **78**, (2008) 041120.
12. U. Seifert, *Rep. Prog. Phys.* **75**, (2012) 126001.
13. M. Baiesi and C. Maes, *New J. Phys.* **15**, (2013) 013004.
14. R. K. P. Zia, E. L. Praestgaard, and O. G. Mouritsen, *Am. J. Phys.* **70**, (2002) 384.
15. S. Leitmann, and T. Franosch, *Phys. Rev. Lett.* **111**, (2013) 190603.
16. U. Basu and C. Maes, *J. Phys. A: Math. Theor.* **47**, (2014) 255003.
17. O. Bénichou, P. Illien, G. Oshanin, A. Sarracino, and R. Voituriez, *Phys. Rev. Lett.* **113**, (2014) 268002.
18. M. Baiesi, A. L. Stella, and C. Vanderzande, *Phys. Rev. E* **92**, (2015) 042121.
19. O. Bénichou, P. Illien, G. Oshanin, A. Sarracino, and R. Voituriez, *Phys. Rev. E* **93**, (2016) 032128.
20. A. Ros, R. Eichhorn, J. Regtmeier, T. T. Duong, P. Reimann and D. Anselmetti, *Nature* **436**, (2005) 928.
21. M. Kostur, L. Machura, P. Hänggi, J. Luczka, and P. Talkner, *Physica A* **371**, (2006) 20.
22. L. Machura, M. Kostur, P. Talkner, J. Luczka and P. Hänggi, *Phys. Rev. Lett.* **98**, (2007) 040601.
23. D. Speer, R. Eichhorn, and P. Reimann, *EPL* **79**, (2007) 10005.
24. R. Eichhorn, J. Regtmeier, D. Anselmetti, and P. Reimann, *Soft Matter* **6**, (2010) 1858.
25. M. R. Maxey, *Phys. Fluid.* **39**, (1987) 1915.
26. J. Rubin, C.K.R.T. Jones, and M. Maxey, *J. Nonlinear Sci.* **5**, (1995) 337.
27. J. C. H. Fung, *J. Aerosol Sci.* **28**, (1997) 753.
28. J.-R. Angilella, *Phys. of Fluids* **19**, (2007) 073302.
29. J. Bec, L. Biferale, M. Cencini, A. Lanotte, S. Musacchio and F. Toschi, *Phys. Rev. Lett.* **98**, (2007) 084502.
30. E. Calzavarini, M. Cencini, D. Lohse and F. Toschi, *Phys. Rev. Lett.* **101**, (2008) 084504.
31. A. Sarracino, F. Cecconi, A. Puglisi, and A. Vulpiani, *Phys. Rev. Lett.* **117**, (2016) 174501.
32. R. L. Honeycutt, *Phys. Rev. A* **45**, (1992) 600.
33. N. Fenichel, *J. Differential Equations* **31**, (1979) 5198.
34. T.J. Burns, R.W. Davies, and E.F. Moore, *J. Fluid Mech.* **384**, (1999) 1.
35. D. Speer, R. Eichhorn, and P. Reimann, *Phys. Rev. E* **76**, (2007) 051110.
36. S. Colabrese, K. Gustavsson, A. Celani, and L. Biferale, *Phys. Rev. Lett.* **118**, (2017) 158004.